Dear Author,

Please, note that changes made to the HTML content will be added to the article before publication, but are not reflected in this PDF.

Note also that this file should not be used for submitting corrections.

AUTHOR QUERY FORM

ELSEVIER	**Journal: RSE** **Article Number: 9316**	**Please e-mail or fax your responses and any corrections to:** **Subramaniam, Harinath** **E-mail: Corrections.ESCH@elsevier.spitech.com** **Fax: +1 619 699 6721**

Dear Author,

Please check your proof carefully and mark all corrections at the appropriate place in the proof (e.g., by using on-screen annotation in the PDF file) or compile them in a separate list. Note: if you opt to annotate the file with software other than Adobe Reader then please also highlight the appropriate place in the PDF file. To ensure fast publication of your paper please return your corrections within 48 hours.

For correction or revision of any artwork, please consult http://www.elsevier.com/artworkinstructions.

We were unable to process your file(s) fully electronically and have proceeded by

☐ Scanning (parts of) your article ☐ Rekeying (parts of) your article ☐ Scanning the artwork

Any queries or remarks that have arisen during the processing of your manuscript are listed below and highlighted by flags in the proof. Click on the 'Q' link to go to the location in the proof.

Location in article	Query / Remark: click on the Q link to go Please insert your reply or correction at the corresponding line in the proof
Q1	Your article is registered as a regular item and is being processed for inclusion in a regular issue of the journal. If this is NOT correct and your article belongs to a Special Issue/Collection please contact h.subramaniam@elsevier.com immediately prior to returning your corrections.
Q2, Q5	Please confirm that given names and surnames have been identified correctly.
Q3	Citation "Frolking et al. 2009" has not been found in the reference list. Please supply full details for this reference.
Q4	Citation "Azimuth-Systems, 2011" has not been found in the reference list. Please supply full details for this reference.
Q6	Please check the page range in Ref. Gower, 1966.
Q7	Please check the page range in Ref. Simpson, 1949 Please check this box if you have no corrections to make to the PDF file. ☐

Thank you for your assistance.

Remote Sensing of Environment xxx (2015) xxx

Contents lists available at ScienceDirect

Remote Sensing of Environment

journal homepage: www.elsevier.com/locate/rse

Highlights

Remote Sensing of Environment xxx (2015) xxx–xxx

Hyperspectral remote sensing of peatland floristic gradients

A. Harris [a,*], R. Charnock [b], R.M. Lucas [c]

[a] Geography, School of Environment, Education and Development, University of Manchester, Manchester M13 9PL, United Kingdom
[b] Department of Geography and Earth Sciences, Aberystwyth University, Aberystwyth, Ceredigion SY23 3DB, United Kingdom
[c] School of Biological, Earth and Environmental Sciences, University of New South Wales, New South Wales 2052, Australia

- Hyperspectral data were used to map peatland floristic gradients.
- The same analyses were performed at two hierarchical levels of species aggregation.
- Transitions in species composition and PFTs were quantified using Isomap.
- Ordination scores were modelled and mapped from spectral reflectance using PLSR.
- The method does not require the identification of unique spectral signatures.

http://dx.doi.org/10.1016/j.rse.2015.01.029
0034-4257/

Please cite this article as: Harris, A., et al., Hyperspectral remote sensing of peatland floristic gradients, *Remote Sensing of Environment* (2015), http://dx.doi.org/10.1016/j.rse.2015.01.029

Remote Sensing of Environment xxx (2015) xxx–xxx

Contents lists available at ScienceDirect

Remote Sensing of Environment

journal homepage: www.elsevier.com/locate/rse

Hyperspectral remote sensing of peatland floristic gradients

A. Harris [a,*], R. Charnock [b], R.M. Lucas [c]

[a] Geography, School of Environment, Education and Development, University of Manchester, Manchester M13 9PL, United Kingdom
[b] Department of Geography and Earth Sciences, Aberystwyth University, Aberystwyth, Ceredigion SY23 3DB, United Kingdom
[c] School of Biological, Earth and Environmental Sciences, University of New South Wales, New South Wales 2052, Australia

ARTICLE INFO

Article history:
Received 24 March 2014
Received in revised form 20 November 2014
Accepted 26 January 2015
Available online xxxx

Keywords:
Peatland
Vegetation
Ordination
Partial least squares regression
Hyperspectral
Plant functional type

ABSTRACT

Previous studies have shown that the floristic composition of northern peatlands provides important information regarding ecosystem processes and their responses to environmental change. Remote sensing is the most expeditious method of obtaining floristic information at landscape and regional scales, but the spatial complexity of many northern peatlands and the spectral similarity of a number of peatland vegetation species is such that the success of traditional methods of vegetation classification is often limited. Here, we assessed whether ordination and regression analysis may be a useful alternative method for mapping peatland plant communities from remote sensing data. We used isometric feature mapping (Isomap) to describe the community structure of the peatland vegetation and related the identified continuous floristic gradients to hyperspectral imagery (AISA Eagle) using partial least squares regression (PLSR). We performed the same analysis at two hierarchical levels of species aggregation in order to map continuous gradients in the composition of both species and plant functional types (PFTs), the latter of which is the most widely used level of aggregation in northern ecosystems. Isomap was able to transfer 82% and more than 96% of the observed ground-based observations to the ordination space for plots characterised by species and PFT; respectively. The modelled floristic gradients showed good agreement with ground-based species and PFT observations although the strength of the agreement was proportional to the amount of floristic variation explained by each ordination axis (r^2_{val} = 0.74, 0.45 and 0.30 for the first three ordination axes and r^2_{val} = 0.68 and 0.66 for the first two ordination axes; for species and PFT floristic gradients respectively). We also found that how a PFT is defined has an important influence on the success with which it can be mapped. The resultant mapped floristic gradients enabled visualisation of homogeneous vegetation stands, heterogeneous mixtures of different key species and PFTs, and the presence of continuous and abrupt floristic transitions, without the need for unique spectral signatures or the collection of data characterising ancillary environmental variables.

1. Introduction

Peatlands represent a diverse array of wetlands that accumulate partially decomposed organic material. Whilst they may only cover a small proportion (~3%) of the Earth's land surface, these ecosystems are hugely important in terms of their functional and ecological values. Undisturbed, global peatland systems act as net atmospheric carbon sinks, storing approximately a third of the world's soil organic carbon (Gorham, 1991), the vast majority of which (450–547 GtC) is stored in northern peatlands (those above 45°N; Yu, Loisel, Brosseau, Beilman, & Hunt, 2010). From an ecological perspective, these environments also provide important habitats for a number of rare plant and animal species, to the extent that the ecology of peatlands has received national and global recognition (e.g., the UK Post-2010 Biodiversity Framework, the EU Habitats Directive, the Ramsar Convention on Wetlands, and the Convention on Biological Diversity).

The floristic composition of an ecosystem is closely related to the rate and magnitude of its processes (Díaz & Cabido, 2001; Tilman et al., 1997). Within peatlands, species distributions reflect subtle gradients in water movement and chemistry (Rydin & Jeglum, 2006). However, many peatland species are sensitive to modifications of moisture, temperature and nutrient regimes (Foster, H.E.W., Thelaus, & King, 1993; Minkkinen, Korhonen, Savolainen, & Laine, 2002). Small environmental changes can alter the floristic composition of a peatland, triggering changes in the rates of primary production (Belyea & Malmer, 2004; Bubier, Moore, & Bledzki, 2007; Waddington, Griffis, & Rouse, 1998; Wiedermann, Nordin, Gunnarsson, Nilsson, & Ericson, 2007) and plant litter decomposition (Dorrepaal, Cornelissen, Aerts, Wallen, & Van Logtestijn, 2005), which affect ecosystem carbon dynamics (Strack & Waddington, 2007). Consequently, monitoring the plant species composition of a peatland is important in order to understand the response of these ecosystems to past and current climatic conditions, and to predict the effects of future climate changes (Gray et al., 2013).

The remoteness of many northern peatlands is such that remote sensing provides an expeditious and economical way of supplementing

* Corresponding author.
E-mail address: angela.harris@manchester.ac.uk (A. Harris).

http://dx.doi.org/10.1016/j.rse.2015.01.029
0034-4257/

traditional ground-based observations, which are typically of limited temporal resolution and spatial extent, and are often expensive, logistically difficult and time consuming to collect. Classification or clustering approaches are often used by remote sensing analysts and plant community ecologists to produce maps of plant communities, for example see Turner et al. (2003) and references therein. These methods often result in the production of discrete maps, which create artificial "hard" boundaries between different classified patches. Discrete classifications are particularly problematic for mapping the floristic composition of individual peatlands. Changes in species composition can occur over relatively short distances (~1 m), largely as consequence of hydrology, which results in gradual transitions in species proportions as opposed to clear class boundaries (Harris & Bryant, 2009).

Linear mixture modelling or spectral mixture analysis (SMA; Roberts, Smith, & Adams, 1993) is one of the most widely used methods for continuous mapping of plant assemblages from remotely sensed data. SMA assumes that the spectral signature of a pixel is a linear mixture of different plant community or species classes. However, although the outputs from linear mixture modelling are continuous modelled abundances, the approach still requires that the user pre-define the classes to be modelled, and assumes that it is possible to identify pure regions of each of these classes within the image. The spatial heterogeneity of a peatland surface is such that in practice, these requirements are very difficult to fulfil. Combined ordination and regression approaches have been developed to try and overcome some of the limitations of mapping approaches that require vegetation to be categorised a priori (Schmidtlein, Zimmermann, Schüpferling, & Weiβ, 2007) and the need for homogenous plant coverage at the spatial resolution of the sensor. Typically, ordination methods are used to assign numerical values (i.e., ordination scores) to plot-level species data, which relate to the level of floristic similarity or dissimilarity between plots. The floristic gradients, via their ordination scores, are subsequently related to spectral reflectance through regression modelling. The resulting equations are then applied to the imagery to produce maps of ordination scores, which can be interpreted as continuous floristic gradients (Feilhauer, Faude, & Schmidtlein, 2011; Schmidtlein & Sassin, 2004; Schmidtlein et al., 2007; Thessler, Ruokolainen, Tuomisto, & Tomppo, 2005). This combined ordination–regression approach has been used to map relatively homogenous landscapes such as grasslands (Schmidtlein & Sassin, 2004) but there are limited studies, which utilise this approach for mapping species composition in heterogeneous landscapes (Feilhauer et al., 2011). Few have employed ordination approaches for specifically mapping peatland vegetation (Middleton et al., 2012; Thomas et al., 2002) but those that have often combine traditional ordination techniques (e.g., correspondence analysis or canonical correspondence analysis) with supervised classification (e.g., maximum likelihood classification or support vector machines). There are very few studies that investigate the potential of ordination–regression methods for continuous mapping of peatland floristic composition (Schmidtlein et al., 2007) and none that have used this approach for mapping peatland plant functional types (PFTs).

Whilst plant species composition can provide important information regarding ecological processes within individual peatlands (Bubier, 1995; Bubier, Moore, & Crosby, 2006; Dias, Hoorens, Van Logtestijn, Vermaat, & Aerts, 2010) and are important for environmental managers, species pools may not be consistent across regions and thus identification of taxonomic plant assemblages may not be the most useful for comparing the influence of environmental perturbations across large spatial extents and between peatlands (Gray et al., 2013; van Wijk et al., 2004; Walker et al., 2006). Instead, PFTs created through the grouping of species into functional groups, which reflect function–process–vegetation relationships, are often used to model the responses of peatlands to environmental change and are heavily used for carbon modelling in northern biomes (Gray et al., 2013; Kuiper, Mooij, Bragazza, & Robroek, 2014; Sloan, Fletcher, Press, Williams, & Phoenix, 2013; Ward, Bardgett, McNamara, & Ostle, 2009). Shrubs, graminoids (sedges, rushes, grasses), bryophytes (nonvascular plants such as mosses), lichens, forbs (other herbaceous plants) and trees are all found in peatlands, although shrubs, graminoids and bryophytes are often the three most dominant PFTs (Frolking et al. 2009). Each PFT represents a group of plants with common structural and functional traits (Gitay & Noble, 1997; e.g., architectures, biochemistry, leaf construction and water content). In northern peatlands, the fractional cover of PFTs, particularly bryophytes, graminoids and shrubs, provide an indication of the current carbon sequestration potential, whereas changes in the fractional cover may provide an early warning of future changes in carbon balance (Schaepman-Strub, Limpens, Menken, Bartholomeus, & Schaepman, 2009). One of the difficulties in using remote sensing to map continuous gradients in PFT as opposed to species composition, as discussed previously, is that individual plant species need to be categorised into pre-defined classes. Traditional image classification methods can be used to group species into PFT classes ex post through post-classification operations. However, direct mapping of PFTs may facilitate more rapid collection of field data to complement remotely sensed imagery, because identifying PFTs is likely to be simpler than identification at the species level. Furthermore, discrepancies between surveys undertaken by different individuals are likely to be minimised as the level of classification required is more generalised (Hearn et al., 2011). The spatial heterogeneity in species composition found in many northern peatlands is such that vegetation sampling plots of just 1 m^2 will often contain multiple PFTs.

There are very few studies that specifically attempt to directly map peatland PFTs from remote sensing data (Cole, McMorrow, & Evans, 2014; Schaepman-Strub et al., 2009; Schmidtlein, Feilhauer, & Bruelheide, 2012), primarily because of the difficulties involved in identifying characteristic spectral signatures using traditional spectral- or pixel-based approaches. The main method used is SMA (e.g., Schaepman-Strub et al., 2009), but difficulties occur in identifying representative and separable endmember spectra for each of the key PFTs; and regression modelling based on direct empirical relationships between PFT percentage coverage and reflectance, but such method can prove to be problematic when mapping locations where the coverage of a PFT is low because of the presence of zeros in the regression models (Cole et al., 2014). Even though there are a limited number of PFTs commonly found within peatlands, we suggest that mapping PFT gradients may result in better models than those derived from single PFTs because gradient positions (i.e., where a plot lies along a floristic gradient) are inherently less variable than individual cover values (Schmidtlein & Sassin, 2004), especially in degraded peatlands or where restoration efforts are under way. A slightly different approach to mapping peatland PFTs was undertaken by Schmidtlein et al. (2012) who used hyperspectral data and partial least squares regression (PLSR; Wold, Ruhe, Wold, & Dunn, 1984) to successfully model the spatial distribution of PFTs based on reflectance and plant strategy scores (Grime, 1974), which were assigned to species level data. However, comparison between the regression methods of Schmidtlein et al. (2012) and the other studies is somewhat hampered by differing definitions of peatland PFTs, which are often based upon the plant functions of most interest for a given study (Ustin & Gamon, 2010).

The aim of this paper is to explore the utility of hyperspectral data for peatland monitoring. Specifically we determine the answer to three key questions, namely: 1. Can the novel ordination method of isometric feature mapping (Isomap) be used to quantify transitions in vegetation composition in an ombrotrophic peatland complex? 2. Can partial least-squares regression (PLSR) be used to effectively model ordination scores from spectral reflectance data for discriminating peatland floristic gradients? 3. Can a combined Isomap-PLSR approach be used to map peatland floristic gradients from hyperspectral imagery? Given the requirement for mapping of plant assemblages at the species level and of PFTs (determined by the scale of the application), this is the first study to assess whether such an approach can be used to model both the spatial variation in species composition of plant assemblages,

Please cite this article as: Harris, A., et al., Hyperspectral remote sensing of peatland floristic gradients, *Remote Sensing of Environment* (2015), http://dx.doi.org/10.1016/j.rse.2015.01.029

and gradient transitions in the proportional coverage of PFTs. As the species and the number of species attributed to individual PFTs may vary between peatlands, we also assess the sensitivity of PFT models to the species assemblages used to define each PFT.

2. Methods

Fig. 1 provides a schematic overview of the methodology used in this study. The methodology consists of 5 main steps: 1. Ordination analysis (i.e., Isomap) is used to depict peatland floristic composition using vegetation coverage data; 2. The spectral signature corresponding to each of the sampling plots is extracted from the AISA Eagle image; 3. The spectral signatures are used to model the position of each sampling plot in ordination space by modelling the ordination scores of each ordination axis in turn (i.e., one model for each ordination axis); and 4. The resultant regression models are subsequently applied to each individual pixel within the hyperspectral image to produce a series of ordination images. Each image represents the ordination score on one of the ordination axes. The grey scale ordination score images are then merged to create a single RGB image. The colour of each pixel represents the position of that pixel in the ordination space and thus indicates the species composition present. The same procedure is used to map the floristic gradient of peatland species and plant function types (PFTs).

2.1. Study area

The study area is Cors Fochno (Borth bog), which is an ombrotrophic (i.e., rain-fed) peatland located on the West coast of Wales, UK (52°32′ N, 04°00′W). Mean annual rainfall at the site is approximately 1220 mm, with the majority (60–70%) falling between October and February. The central dome of the peatland has a defined hummock-hollow microtopographical structure and is one of only a few UK bogs that may be considered as representative of ombrotrophic northern peatland complexes more generally. The active bog dome is characterised by *Sphagnum* mosses (e.g., *Sphagnum pulchrum*, *Sphagnum cuspidatum*, *Sphagnum magellanicum* and *Sphagnum papillosum*), interspersed with white beak-sedge (*Rhynchospora alba*), common cotton grass (*Eriophorum angustifolium*), bog rosemary (*Andromida polyfolia*) and heather (*Calluna vulgaris*). Bog myrtle (*Myrica gale*), hare's tail cotton grass (*Eriophorum vaginatum*), bog asphodel (*Narthecium ossifragum*) and sundew (*Drosera* sp.) are also commonly found on the central dome, whereas purple moor grass (*Molinia caerulea*), reeds and rushes (e.g., *Phragmites australis*, *Juncus maritimus* and *Schoenus nigricans*) are found at the more disturbed bog margins.

2.2. Vegetation survey

Species composition data were collected coincident with the airborne flight campaign in June 2009 and additional vegetation plots were sampled during the summers of 2011 and 2013. The floristic composition of the peatland did not change considerably during this period of time. Species coverage was estimated from a total of 86 vegetation plots within the selected AISA Eagle flight line using a 2 × 2 m sampling frame (Fig. 2). Total plant coverage in each plot summed to 100%. Estimations of the fractional coverage of PFTs were derived from grouping the species level data into one of five widely recognised peatland PFTs; namely bryophytes, graminoids, shrubs, forbs and lichens (Table 1). Each plot was geo-located using a Leica SR20 differential GPS with sub-metre accuracy.

2.3. Airborne data acquisition and pre-processing

Airborne hyperspectral AISA Eagle data (Specim Ltd., Oulu, Finland) were acquired over the study area by the Natural Environment Research Council (NERC) on June 21st 2009 under clear cloud free conditions. AISA Eagle is a 12-bit pushbroom sensor with 252 narrow spectral bands (maximum of 2.9 nm FWHM) covering the visible (VIS) and near-infrared (NIR) regions of the electromagnetic spectrum. The composite of all flight lines covered the entire length and breadth of the site and consisted of 8 lines of imagery and were collected with a spatial resolution of 0.5 m at nadir. However, only a single line of the imagery was used in this study since all the vegetation plots were aligned within the primary flight line to minimise view angle variations. The primary flight line covered a large proportion of the primary dome and was representative of the vegetation composition and structure found across the peatland as a whole.

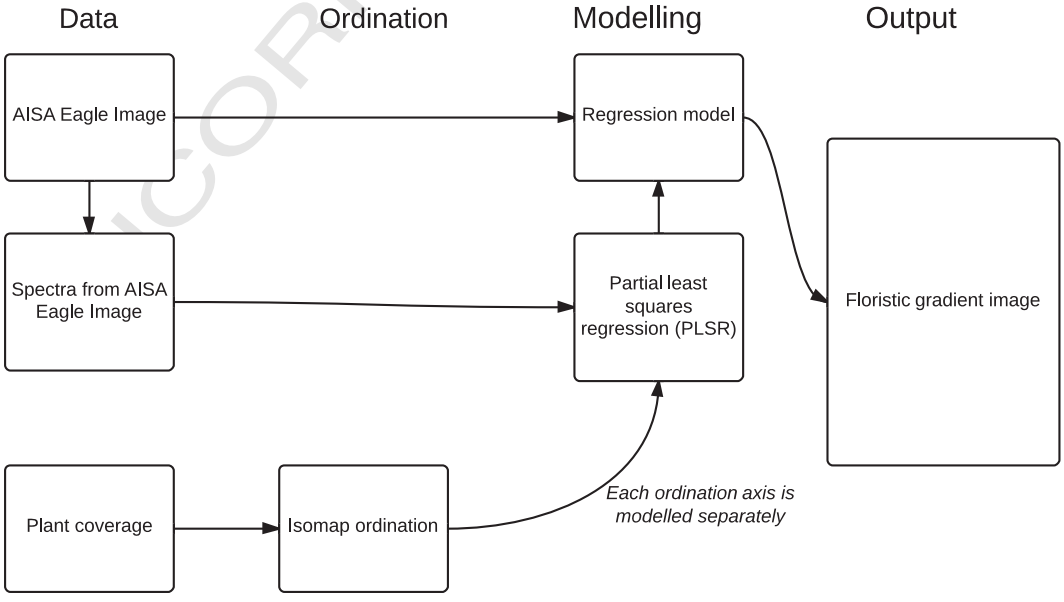

Fig. 1. A schematic overview of the methodology used in this study. Ordination analysis using Isomap was used to depict peatland floristic composition using ground-based plant coverage data. The spectral signature of each of the coverage plots was extracted from the AISA Eagle image. The spectral signatures were then used to model the position of each sampling plot in ordination space by modelling the ordination scores of each ordination axis in turn using partial least squares regression (PLSR). Spatial mapping of each individual ordination axis was achieved by applying the resultant regression models to the AISA image. The same procedure was used to map floristic gradient of peatland species and plant function types (PFTs).

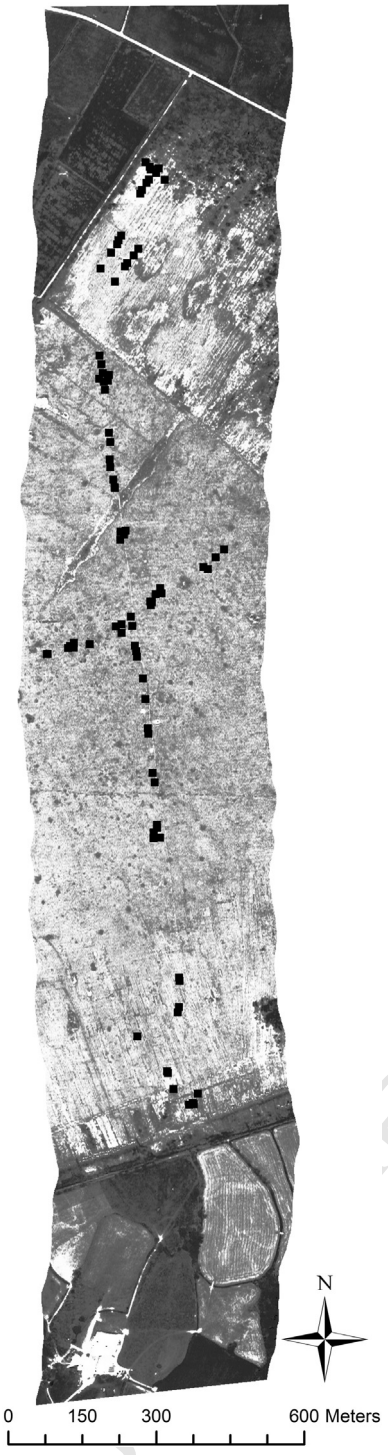

Fig. 2. The distribution of field sampling plots (2 × 2 m) within the hyperspectral flight line. A normalised difference vegetation index image is used as the background image.

The airborne imagery were delivered in radiometrically calibrated Hierarchical Data Format (HDF) and were subsequently geometrically corrected for pitch, roll and yaw effects using the NERC software AZGCORR (Azimuth-Systems, 2011). The software employed aircraft position and attitude data, along with a combined LiDAR and NextMap Digital Elevation Model, to correct the data to the UK national grid using a nearest-neighbour interpolation algorithm. This resulted in an output pixel size of 1 m. The output data were tested for geometric error using a combination of vector overlays from the UK Ordnance Survey (OS) standard map products and a high spatial resolution orthorectified aerial photograph. The at-sensor radiances were atmospherically corrected to surface reflectance using the Fast Line-of-Sight Atmospheric Analysis of Spectral Hypercubes (FLAASH) module in RSI ENVI (v.4.8). FLAASH is a physics-based atmospheric correction model based upon the widely-used and well-validated MODTRAN4 (MODerate resolution atmospheric TRANsmission) radiative transfer code developed by Spectral Sciences Incorporated (Matthew et al., 2000). Water vapour was retrieved on a pixel by pixel basis using the water absorption feature located at 820 nm. The average water vapour modelled by FLAASH across the image was within 0.5 cm (~15%) of that recorded by the Microtops II sunphotometer in the field.

A minimum noise fraction transformation (MNF) was applied to segregate noise within the data (Green, Berman, Switzer, & Craig, 1988). MNF bands that did not contain any coherent spatial information and were judged to be composed predominantly of noise (through coincident examination of the MNF images and associated eigenvalues) were removed and an inverse MNF transform was performed on the remaining bands. A subsequent visual inspection of a selection of spectral profiles revealed the continued presence of several noisy spectral bands (primarily located at the extremes of the sensor's wavelength range). These bands were removed from the image leaving 209 spectral bands across the following ranges: 450–755 nm, 772–928 nm and 957–987 nm. To minimise the influence of geometric errors, the hyperspectral image was smoothed using a 3-by-3 median filter prior to the extraction of the reflectance spectrum of each sampling plot.

Table 1
Key species surveyed and their equivalent plant functional type (PFT).

Plant functional type (PFT)	Key species
Bryophytes	*Sphagnum* spp., *Hypnum jutlandicum*, *Aulacomnium palustre*, *Camplyopus introflexus*, *Cepridozia bicuspidate*, *Dicronium scoparium*, *Cephalozia connivens*, *Kurzia pauciflora*, *Odontoschisma sphagni*
Graminoids	*Rhyncospera alba*, *Eriophorum* spp., *Molinia caerulea*, *Trichopherum cepitosa*, *Narthecium ossifragum*, *Phragmites australis*
Shrubs	*Calluna vulgaris*, *Erica tetralix*, *Myrica gale*, *Vaccinium myrtillus*
Forbs	*Andromeda polifolia*
Lichens	*Cladonia* spp.

2.4. Data analysis

2.4.1. Ordination

Isometric feature mapping (Isomap; Tenenbaum, de Silva, & Langford, 2000) was used to describe the community structure of the peatland vegetation. Isomap is particularly useful for extracting floristic gradients in communities with a high beta-diversity (De'ath, 1999; Minchin, 1987) and may be particularly useful for peatland sites where pairs of sample plots may not share any species because of the vegetation heterogeneity caused by differences in the position of the water table. Species composition data were first transformed into an inter-plot dissimilarity matrix using Bray–Curtis dissimilarities. The Bray–Curtis dissimilarity ranges between 0 and 1, where a value of 1 means that plots share all of their species, and a value of 0 indicates that plots have no species in common. The basic idea of Isomap is to measure dissimilarity distances using a single distance measure for plots that are within a threshold distance, and to use geodesic distances between more distant (i.e., dissimilar) plots. The Bray–Curtis dissimilarity matrix is used to identify k nearest neighbours for each plot. A web of connections between plots is subsequently formed by connecting each plot with its k nearest neighbours. The shortest path along the web is then found for each plot pair and a new matrix of pair-wise geodesic floristic distances is created (Tenenbaum et al., 2000). Classic multidimensional scaling (CMDS; Gower, 1966) is subsequently performed on the geodesic distances to transfer them to a lower dimensionality.

The k value determines the possible paths through the web and thus the optimal value of k is the smallest possible value that leads to a completely connected web and that transfers the most variance (i.e., variability in species composition) to a low dimensional ordination. The distances between a sample and its nearest-neighbour remain linear thus optimum solutions with high k values indicate high linearity in the data whereas low k values suggest nonlinearity. In the present study, the optimal value of k was determined as the value that resulted in the Isomap solution that transferred the largest amount of original variation in the vegetation data to the Isomap ordination space (Feilhauer et al., 2011). Isomap was implemented in the R statistical environment (R Development Core Team, 2012) using the vegan package (Oksanen et al., 2013).

Ordinations were undertaken on the original species data and after the species in each plot were aggregated to one of five recognised peatland PFTs; namely bryophytes, graminoids, shrubs, lichens and forbs. To assess the sensitivity of the ordination, and thus the subsequent modelling, to the number of species included within each PFT we created two PFT datasets, the first utilised all sampled plots and the second used a less species diverse sub-sample where only plots with a Simpson diversity Index (Simpson, 1949) value less than 0.7 were used in the conversion of species to PFT. The first three dimensions of the Isomap space were used to map species composition, whereas only the first two Isomap dimensions were used to map gradient transitions in the proportional coverage of PFTs (see Section 3).

2.4.2. Regression analysis

Partial least squares regression (PLSR) was used to model the relationships between the ordination scores derived from each ordination axis and the reflectance data. PLSR overcomes the problem of multicollinearity among spectral bands by transferring the information content of the spectral bands to independent latent variables (LV), but unlike principal component regression (PCR), the LVs are also optimised to represent the response variable (i.e., the modelled floristic gradient).

Each ordination axis was modelled separately and validated by using leave-one-out cross-validation (LOOCV) where a number of sub-models are computed in which all samples are left out one by one for validation. To avoid model over-fitting, as a consequence of the use of too many latent variables, LOOCV was repeated as the number of LVs was increased and the model with the number of LVs where the root-mean-squared-error (RMSE) approaches a first minimum was selected. Model performance can further be enhanced through the proper selection of variables (Mehmood, Liland, Snipen, & Sæbø, 2012). To further optimise the model we performed a backward selection of the predictors (i.e., spectral bands), which was based on a combination of variable importance in the projection (VIP; Chong & Jun, 2005), significance in jack-knifing or removal of correlated bands, starting at local maxima in weighted regression coefficients (Schmidtlein et al., 2012). The backward selection procedures were undertaken through an automated iterative search using the autopls package (Schmidtlein et al., 2012) implemented in R (R Development Core Team, 2012).

The resultant regression models, one for each ordination axis, were applied to the hyperspectral image to predict ordination scores for each individual peatland pixel, resulting in 3 grey-scale images for the prediction of species composition (i.e., 3 ordination axes) and 2 grey-scale images for the prediction of PFT (i.e., 2 ordination axes). The species composition data were subsequently merged to create a RGB composite to facilitate interpretation of relative positions in ordination space, where each colour in the composite represents the position of a pixel in the ordination space and thus a specific species composition (e.g., Feilhauer et al., 2011; Schmidtlein et al., 2007).

The reliability of the floristic gradient maps was examined by assessing the representativeness of the field sampling data. We calculated distances between the predicted ordination scores of each map pixel and the nearest-neighbour sample plot in the Isomap ordination space. Small distances indicate that the predicted species composition was found within the sampling data, whereas larger distances indicate that the image reflectance was not well characterised by the sampling plots and thus there is greater uncertainty in the prediction (Feilhauer et al., 2011).

3. Results

3.1. Can isometric feature mapping (Isomap) be used to quantify transitions in vegetation composition in an ombrotrophic peatland complex?

A total of 49 species were recorded across the 86 field plots. The number of species per plot ranged between 3 and 21 (mean = 9). A k value of 46 transferred the maximum amount of floristic variation (82%) to the three Isomap axes. Increasing the number of axes to 4 only increased the explained floristic variation by 3% and so a 3 axes model was chosen as the preferred solution.

Fig. 3 illustrates the distribution of sampling plots in the Isomap ordination space. The dominant species found within each plot were used as a factor variable to help description of the species occupying different parts of the ordination space and their centroids were plotted on the ordination graphs, but these data were not used in the actual ordination or in any further analysis. The largest floristic differences were reflected along the first Isomap axis. Plots with low axis 1 scores were dominated by bog mosses such as *Sphagnum* spp. and *Hypnum jutlandicum* whereas plots with the highest scores were dominated by graminoid species such as *M. caerulea*, which is often found at the bog margins and where drainage has occurred. Shrubs such as *C. vulgaris*, which are typically found in drier regions of the peatland, were indicative of low axis 2 scores and intermediate access 1 scores, whereas at the opposite end of axis 2 and with high axis 1 scores, we found species such as *S. pulchrum* and *R. alba*, which are frequently found on moist lawns and at the edges of bog pools. Axis 3 indicated a transition from graminoid communities dominated by *Eriophorum* spp. through to shrub communities dominated by *C. vulgaris* and *M. gale* and the extremes of axis 3 were dominated by bog mosses and lichens such as *Sphagnum* spp. and *Cladonia portentosa*.

Each species in the 86 sampling plots was subsequently allocated to one of the PFTs identified across the peatland. This lead to 26 species being defined as bryophyte, 7 species of graminoid, 7 forbs, 5 lichen species and 4 species classed as shrubs. Between 3 and 21 species were included within any single plot (mean = 9). The coverage of forbs and lichens was low within individual plots and across the site as a whole thus the plots predominantly contained bryophytes, shrubs and graminoids.

To assess the impact that the number of species included within a PFT had upon the ordination result and subsequent modelling, the ordination analysis was performed on the full dataset (n = 86) and then repeated after the exclusion of particularly species diverse sampling plots (Simpsons index > 0.7). The exclusion resulted in a subset of 52 plots containing a total of 28 species. The number of species per plot ranged between 1 and 13 (mean = 5). Only 1 species from each of the shrub and graminoid PFTs (*Vaccinium myrtillus* and *Trichopherum cepitosa*; respectively) was removed but the number of bryophyte species was reduced by 50% to 13; the vast majority of the species removed were generalist bryophytes (e.g., *Aulacomnium palustre*, *Camplyopus introflexus*, *Cepridozia bicuspidate* and *Dicronium scoparium*), indicating that in contrast to the graminoid and shrub PFTs, the species of the bryophyte PFT did not necessarily occupy similar ecological niches to one another. The revised bryophyte PFT was dominated by *Sphagnum* mosses (9 species) and also included *H. jutlandicum* and a number of liverworts (*Cephalozia connivens*, *Kurzia pauciflora* and *Odontoschisma sphagni*). One lichen species and 5 forbs also remained but only the lichen species (*C. portentosa*) had greater than 5% coverage within any single plot.

Results from both of the PFT ordinations (n = 86 and n = 52) are shown in Fig. 4. Two axes were able to explain 96.9% and 98.9% of the

Please cite this article as: Harris, A., et al., Hyperspectral remote sensing of peatland floristic gradients, *Remote Sensing of Environment* (2015), http://dx.doi.org/10.1016/j.rse.2015.01.029

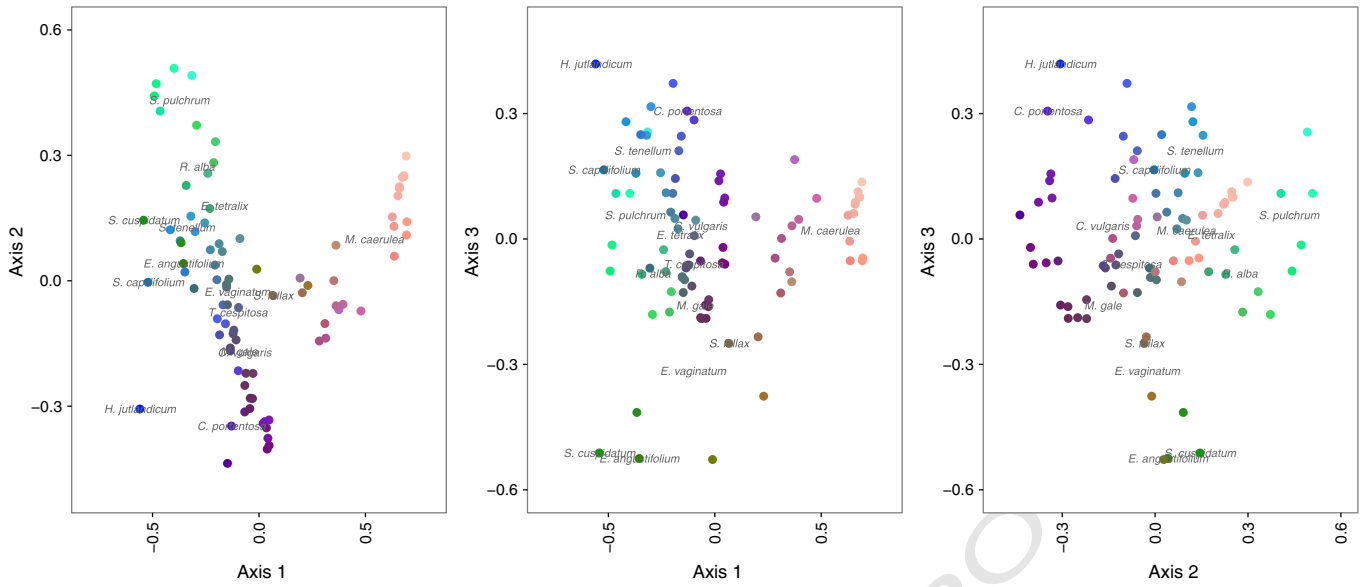

Fig. 3. The distribution of sampling plots characterised by species in three-dimensional ordination (Isomap) space. The colour of each plot represents its position in ordination space (axis 1 = red, axis 2 = green, axis 3 = blue). Plots close together have similar species compositions. To further aid visual interpretation, the dominant species found within each plot is plotted as a centroid and labelled with the species name, which indicates the average position that is predicted for plots with the same dominant species. (For interpretation of the references to colour in this figure legend, the reader is referred to the web version of this article.)

variation within the original Bray–Curtis dissimilarity matrix for the full dataset and the sub-sampled dataset respectively (k = 40 and k = 39; respectively). Differentiation between plots was greatest along axis 1 for both datasets, although the distribution of plots in ordination space was somewhat different. For the full dataset, low axis 1 scores were indicative of shrub-dominated communities often with a high coverage of *C. vulgaris* (Fig. 4a). High axis 1 scores reflected graminoid-dominated communities containing *M. caerulea*. Plots with high bryophyte coverage had similar axis 1 scores to plots where proportions of shrubs and graminoids were similar but higher scores than either in axis 2. Low axis 2 scores were thus characteristics of shrub and graminoid communities with low or no bryophyte coverage.

The ordination plot for the PFT subset data clearly differentiated communities with high shrub coverage (Fig. 4b). Plots with the highest scores along the first axis were indicative of plots with 100% shrub coverage. Intermediate axis 1 scores and high axis 2 scores were associated with plots containing a mixture of graminoids and shrubs; the higher the score on axis 2 the greater the proportional cover of shrubs within the plot. The second axis reflected a transition in PFTs from plots containing pure bryophyte coverage (i.e., low scores on both axes 1 and 2) to those completely dominated by graminoid species (i.e., low scores on axis 1 but high axis 2 scores). Plots containing mosaics of shrubs and bryophytes were not present in the subset data as these plots were the most heterogeneous and many contained generalist bryophyte species. The bryophyte PFT was thus dominated by *Sphagnum* mosses, which lead to a clearer separation of the three dominant PFTs within the ordination space.

3.2. Can partial least-squares regression (PLSR) be used to effectively model ordination scores from spectral reflectance data for discriminating peatland floristic gradients?

Table 2 summarises the results of the species PLSR modelling. The explanatory power of each model was related to the amount of floristic variation in the original dissimilarity matrix that the corresponding ordination axis was able to explain. The coefficient of determination for the third axis for the species composition model was relatively weak (r^2_{val} = 0.3) but was retained as the RMSE, when expressed as a percentage of the range of axis scores, was similar to that of the first two axes. Fig. 5 shows the cross-validation model fits for each individual axis.

The regression coefficients of the PLSR models indicated that reflectance bands located in the red region of the electromagnetic spectrum (634–680 nm), and specifically those surrounding the chlorophyll absorption feature (675–680 nm), were important for the prediction of all ordination axes. Spectral bands located in the red region had the strongest influence on axis 2 and 3 score predictions whereas NIR bands (957 nm and 987 nm) exhibited the most influence on predicted axis 1 scores. Bands located in the green and yellow regions (546–610 nm), the red-NIR transition or red-edge (719 and 748 nm) and NIR wavelengths also contributed to the prediction of the first two axes. Reflectance in the blue was predominantly used for modelling axis 3 (450–475 nm; respectively) but also contributed to axis 2 (457 nm).

Table 3 summarises the results of the PFT PLSR modelling. Although Isomap was able to explain a similar amount of floristic variation in both the full and the more homogenous subset dataset (Table 3), there were substantial differences in the ability of the models to predict the floristic differences from spectral reflectance.

The explanatory power PLSR for modelling the full dataset was limited to just a single axis of the ordination (r^2_{val} = 0.65 and r^2_{val} = 0.19 for axes 1 and 2, respectively), whereas PLSR was able to predict scores along both ordination axis for the sub-sampled data (r^2_{val} = 0.56 and r^2_{val} = 0.60 respectively). Given the limited ability of the PFT PLSR modelling for predicting floristic variation of the full sampling dataset, which included all 86 sampled plots, further analyses focused on the subset data. Fig. 6 shows the cross-validation model fits for each individual axis for the subset dataset (n = 52). Deviations from the regression line are greatest for low axis 1 scores (Fig. 6a), which represent plots dominated by Bryophytes or Graminoids. Consequently, both PFTs tend to overlap in ordination space along axis 1 (Fig. 4b). Thus, even though these plots have a similar axis 1 score, they are likely to have quite different spectral signatures. Therefore, both axes are required for modelling PFT.

In contrast to the species data, only bands located in the red (646–693 nm), along the red-edge (700–729 nm) and in the NIR (843–982 nm) regions were used to predict ordination scores related

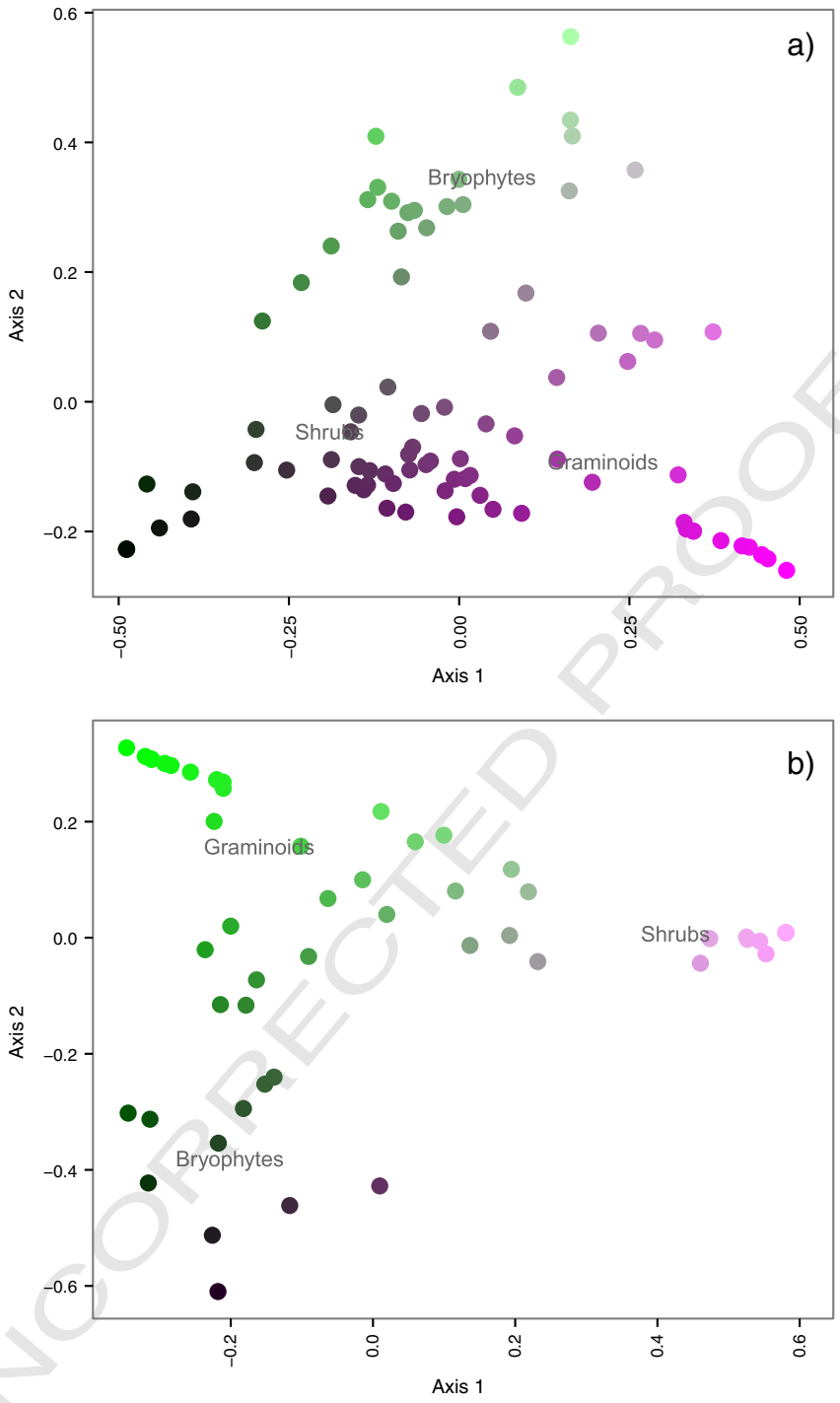

Fig. 4. The distribution of sampling plots characterised by plant functional type (PFT) in two dimensional ordination (Isomap) space; a) all sampled plots (n = 86) and b) only the less species diverse sampling plots (n = 52). The colour of each plot corresponds to its position in the ordination space. Note that because only 2 axes are used, to help visualisation the 1st axis is assigned to both red and blue colour space and the 2nd axis is assigned to green. The dominant PFT found within each plot is plotted as a centroid to help visual interpretation. The centroid indicates the average position that is predicted for plots with the same dominant PFT and is labelled with the name of the PFT. (For interpretation of the references to color in this figure legend, the reader is referred to the web version of this article.)

to the proportional coverage of PFTs. Bands located around the chlorophyll absorption feature (~680 nm) and along the red-edge were used to model both axes. NIR bands that characterised the broad reflectance peak centred at approximately 850 nm were used to model axis 1 scores, whereas the model for axis 2 scores made use of slightly longer wavelengths within the NIR, which characterised either side of the water absorption feature centred at approximately 970 nm.

3.3. Can a combined Isomap–PLSR approach be used to map peatland floristic gradients from hyperspectral imagery?

The PLSR modelling results were used to create maps of each Isomap axis in order to visualise the spatial distribution of peatland species and PFT assemblages across the bog. Each pixel was assigned a colour in RGB space according to the modelled Isomap scores for each ordination axis.

Please cite this article as: Harris, A., et al., Hyperspectral remote sensing of peatland floristic gradients, *Remote Sensing of Environment* (2015), http://dx.doi.org/10.1016/j.rse.2015.01.029

Table 2
Results of the partial least squares regression (PLSR) models for the species-level Isomap ordination axes (R^2_{cal} and R^2_{val} are the R^2 values in the calibration and leave-one-out (LOO) cross-validation; respectively and $RMSE_{cal}$ and $RMSE_{val}$ are the root mean squared error in the calibration and validation data; respectively).

	Axis 1	Axis 2	Axis 3
R^2_{cal}	0.77	0.59	0.39
R^2_{val}	0.74	0.45	0.30
$RMSE_{cal}$	0.17	0.14	0.14
$RMSE_{val}$	0.18	0.17	0.16
No. latent variables	5	10	4
Floristic variation explained by each axis (%)	58.4	12.1	11.2

Table 3
Results of the partial least squares regression (PLSR) models for the PFT Isomap ordination axes for both the full dataset (n = 86) and the subset dataset where only plots with moderate to low floristic diversity (Simpsons index value = <0.7) were included in the analysis (n = 52; R^2_{cal} and R^2_{val} are the R^2 values in the calibration and leave-one-out (LOO) cross-validation; respectively and $RMSE_{cal}$ and $RMSE_{val}$ are the root mean squared error in the calibration and validation data; respectively).

	Full dataset		Subset dataset	
	Axis 1	Axis 2	Axis 1	Axis 2
R^2_{cal}	0.73	0.27	0.68	0.66
R^2_{val}	0.65	0.19	0.56	0.60
$RMSE_{cal}$	0.12	0.18	0.17	0.14
$RMSE_{val}$	0.14	0.19	0.20	0.15
No. latent variables	7	4	6	4
Floristic variation explained by each axis (%)	57.6	39.3	55.8	43.2

Fig. 7 shows the transitions in species composition across the peatland. To aid interpretation, the legend includes a series of ordination diagrams highlighting the distribution of some of the dominant peatland species in the Isomap space and thus enables associations to be drawn between the colours in the image and assemblages of key species. The centre of the bog dome is characterised by a series of *Sphagnum* dominated lawns and pools. In the image these areas are clearly shown as bright green or cyan in colour (Fig. 7d) and are indicative of *S. pulchrum* and *Sphagnum*–*Eriophorum* mosaics (Fig. 7b and c). Drier areas of the peatland are located to the north of the image and along the drainage ditches to the South. Key species found in these locations included *C. vulgaris* and *M. caerulea*, represented by the pink and peach tones. The brown tones, which are interspersed between the *Sphagnum* patches, are indicative of assemblages of *Eriophorum* species, *C. vulgaris* and *E. tetralix*, with slight *Eriophorum* dominance. The darker blue shades within the centre of the bog are representative of species compositions that have a high proportional coverage of *C. vulgaris* and *E. tetralix*, whereas dark green regions contain a higher coverage of *Eriophorum* species.

Fig. 8 maps transitions in the proportion of PFTs. Areas dominated by shrub cover appear in light pink tones (Fig. 8b and c). Higher shrub coverage is evident in drier regions to the north of the draining ditch, which runs from West to East across the peatland surface towards the centre of the image (Fig. 8a). Areas of high graminoid coverage are represented by bright greens and are present in the far North and around the peat cuttings towards the South of the site. These areas of high proportional graminoid coverage correspond well with the mapped coverage's of *M. caerulea* and *C. vulgaris* in the species map (Fig. 7a). The dark purple tones towards the centre of the image highlight areas of high bryophyte density and also correspond well with the *S. pulchrum*-dominated patches identified in the species map (Fig. 7a). Light green tones are indicative of relatively even coverage of graminoids and shrubs.

Uncertainty in the PLSR predictions was ascertained by measuring the distance between each pixel in the image and its nearest-neighbour plot in Isomap ordination space. This measure provides an indication of how closely the vegetation sample data represented the reflectance measures within the image. Uncertainty images for the species and the PFT transition maps are shown in Fig. 9. Distance values for the majority of pixels for both maps were less than 0.1, indicating high certainty. This corresponded to 8% of the length of the first axis, 10.6% of the length of the second axis and 10.5% of the third axis for the species composition map and 10.8% and 10.7% of the length of the first and second axis for the PFT transition map; respectively. Areas with distances greater than 0.2 were more prominent in the species uncertainty image and were predominantly located in the drier outer regions of the bog, where only limited vegetation sampling was undertaken. The lower number of ordination axes used and the generalised nature of the PFT categories resulted in lower prediction uncertainties (Fig. 9b).

4. Discussion

We explored the potential of a combined ordination–regression approach for modelling the spatial distribution of species composition and

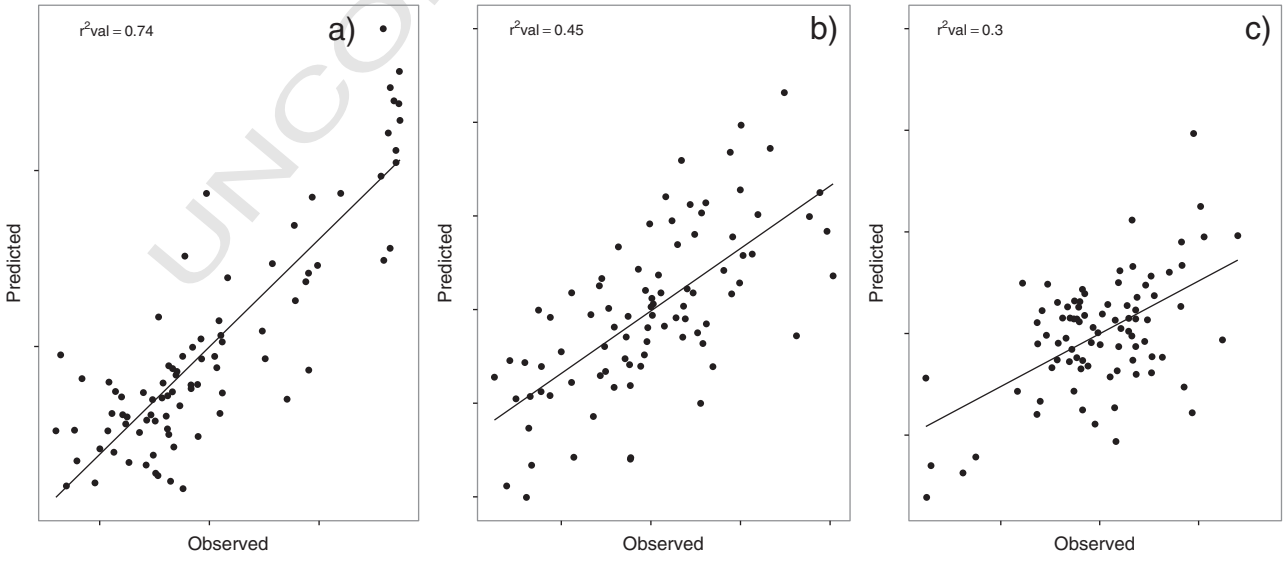

Fig. 5. Partial least squares regression model fits for plots characterised by species (n = 86). The graphs show the relationship between predicted and observed scores for a) axis 1, b) axis 2 and c) axis 3.

Please cite this article as: Harris, A., et al., Hyperspectral remote sensing of peatland floristic gradients, *Remote Sensing of Environment* (2015), http://dx.doi.org/10.1016/j.rse.2015.01.029

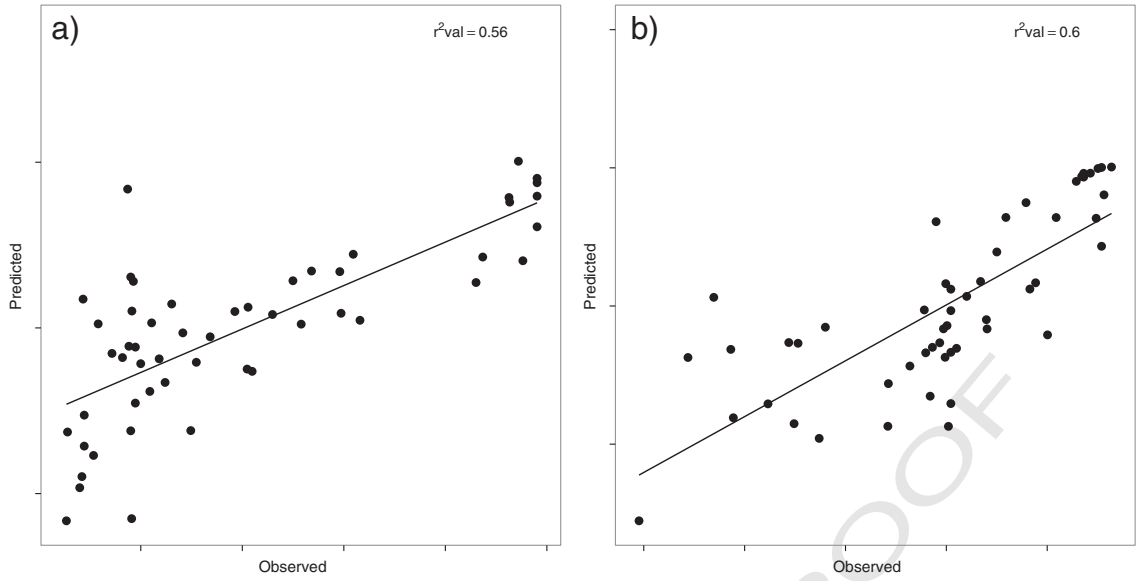

Fig. 6. Partial least squares regression model fits for plots characterised by PFT (n = 52). The graphs show the relationship between predicted and observed scores for a) axis 1 and b) axis 2.

PFT assemblages from remote sensing data. Similar to a number of other studies (e.g., Feilhauer et al., 2011; Mahecha, Martinez, Lischeid, & Beck, 2007; Mahecha & Schmidtlein, 2008), Isomap was able to preserve a high percentage of original variation observed in the original plot-wise dissimilarity matrices for plots characterised by species and PFT (82% and more than 96% of the variation; respectively).

The explanatory power of each of the PLSR models was related to the amount of floristic variation in the original dissimilarity matrix that the corresponding ordination axis was able to explain. Reflectance was always most strongly related (r^2_{val}) to the first Isomap axis. Identification of transitions in the composition of PFTs, which are widely recognised by the peatland biogeochemical community, meant that unlike the mapping of species assemblages, PFT classes were defined a priori based on species groupings. Models will be strongest where the species that determine each PFT have similar morphological and physiological adaptations, which can be linked to optically relevant attributes (Schmidtlein et al., 2012; Ustin & Gamon, 2010). Regression models relating similar ordination scores to very different spectral characteristics, as a consequence of the way in which species are grouped, are likely to perform poorly. This was apparent in our results for the PFT dataset containing all the sample plots, where only the first axis representing floristic differences between shrub and graminoid-dominated mosaics was sufficiently well modelled ($r^2_{val} = 0.67$). Bryophytes were not well modelled (i.e., axis 2) because the category contained a wide range of different species, which occupied different environmental niches (e.g., ranging from very wet to very dry environments) and thus differed in their morphological adaptations and biochemistry, resulting in distinctively different spectral characteristics. Consequently a number of plots, which contained bryophytes, had similar ordination scores because they had a similar composition in terms of the defined PFTs, but the plots differed markedly in their spectral characteristics resulting in the weak regression models reported for axis 2 of the full data set model (Table 3). Other studies have also shown significant differences in the spectral characteristics of wetland mosses, which characterise different environmental niches in relation to moisture availability (Bubier, Rock, & Crill, 1997). The removal of the most species diverse plots resulted in a reduction in the number of bryophyte species such that only moss species with characteristic environmental niches remained. This lead to a slight decrease in the coefficient of determination for axis 1 but the r^2 values during model validation for both ordination axes were >0.5 and thus the model was deemed to be superior. Unlike bryophytes, graminoids and shrubs were well modelled regardless of the level of species diversity within a plot (i.e., for both the full and sub-set datasets), suggesting that differences in the spectral characteristics of species within each of these PFTs was less than the differences observed between them. The slightly lower coefficients of determination of both the species and PFT composition regression models reported here, compared to previous studies that have used a similar ordination–regression approach (Feilhauer et al., 2011; Schmidtlein & Sassin, 2004; Schmidtlein et al., 2007), may be partly a consequence of the relatively short floristic gradient, especially for the PFT ordination, in comparison to those found in other ecosystems.

We used the Euclidean distance between the predicted pixels and the most similar plot from the sampling data as an indication of the uncertainty of the modelling process and how representative the reflectance properties of the field data were in relation to those of the image as a whole. The error maps suggested that the primary bog surface was well characterised by the sampled image spectral data. The sampled image spectra of the vegetation plots were more representative of those found across the entire image when mapping PFT composition due to only using two ordination axes to model 3 PFTs, and thus uncertainties were generally lower than those for the species composition mapping. Areas away from the primary bog were not well sampled, which lead to some of the highest levels of uncertainty. However, in situ observations show that these areas are largely dominated by graminoids, which matches well with both the species composition and PFT transition maps.

The weighted regression coefficients from the PLSR models highlighted differences in the relative importance of regions of the electromagnetic spectrum for modelling species composition and patterns of PFTs. The visible region of the spectrum, which depicts differences in pigmentation and colour, was of particular importance for modelling species compositions but bands located along the red-edge and in the NIR region, which are associated with changes in both chlorophyll content and structure, were often selected by PLSR for modelling the composition of PFTs. A number of spectral bands situated around the NIR water absorption feature (~970 nm) were also important for modelling the transitions in PFT composition. Reflectance at and around the 970 nm absorption feature is related to vegetation moisture content and, in locations occupied by a high coverage of *Sphagnum* moss, can

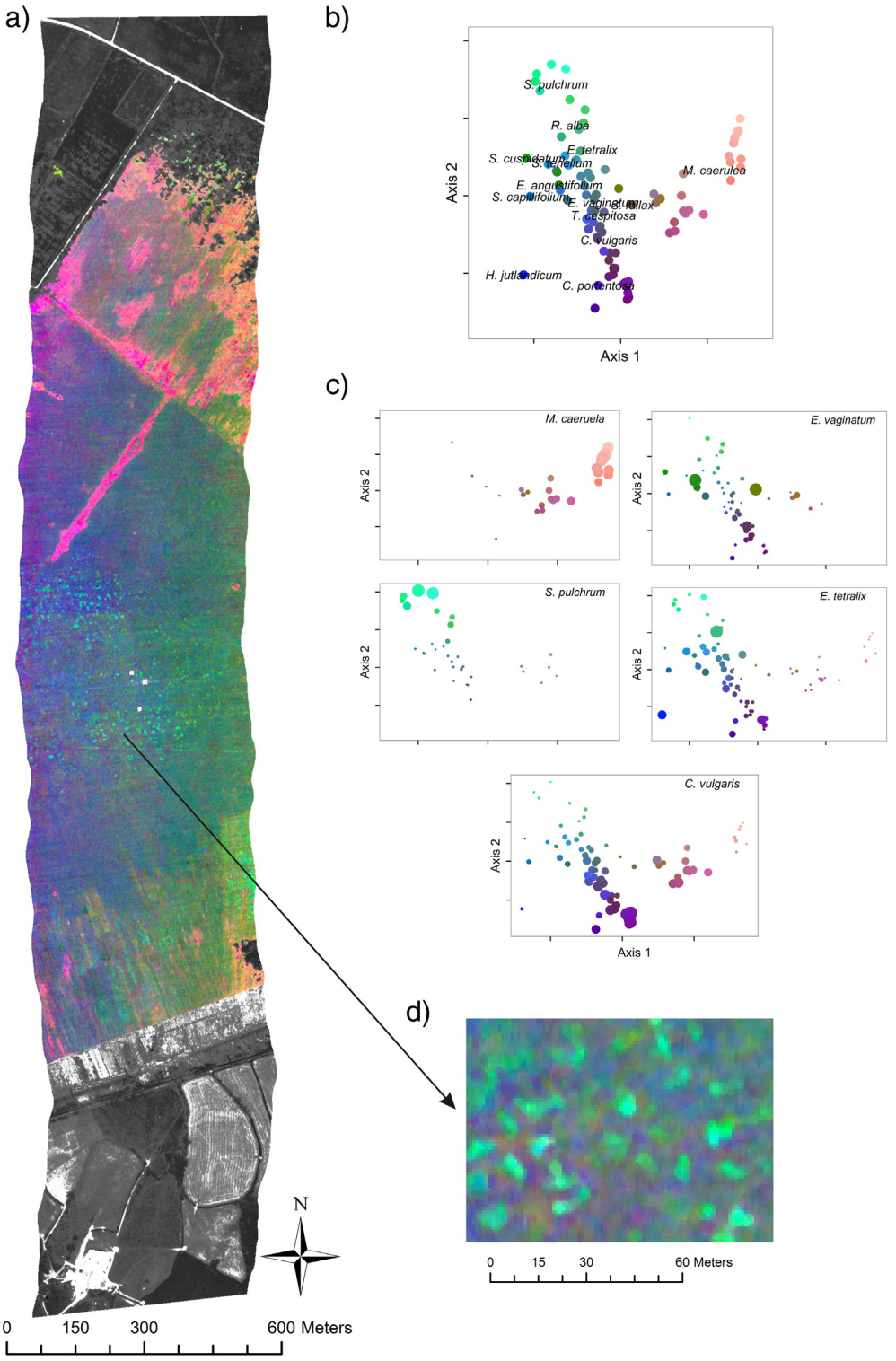

Fig. 7. a) Map of ordination scores representing transitions in peatland species composition (red = axis 1, green = axis 2 and blue = axis 3). Areas surrounding the primary bog are not mapped along with three artificial calibration targets that were also present towards the centre of the image. A normalised difference vegetation index image is used as the background image. Several ordination plots have been included to help interpretation b) indicates the position of individual species in ordination space. The names of some species have been removed for clarity but readers are referred to Fig. 3 for a full depiction of where every species lies in ordination space. The dominant species found within each plot is plotted as a centroid and labelled with the species name; and c) focuses on the position of five common species in ordination space. For each species the size of the circle is representative of the percentage cover of the named species within each field plot. Plots where a given species is not present are not shown; d) is a zoom image of a location on the primary bog surface. The colours in the figure represent the plot (b and c) or pixel locations (a and d) in the full ordination space (although only two axis have been plotted on the graphs for clarity), and thus indicates the species composition present. (For interpretation of the references to color in this figure legend, the reader is referred to the web version of this article.)

be an indicator of near-surface hydrology (Harris, Bryant, & Baird, 2005, 2006). A number of other studies have noted the importance of these spectral regions for identifying peatland PFTs or key PFT species (Bubier et al., 1997; Cole et al., 2014; Schaepman-Strub et al., 2009) and for mapping similar PFTs in tundra regions (Huemmrich et al., 2013).

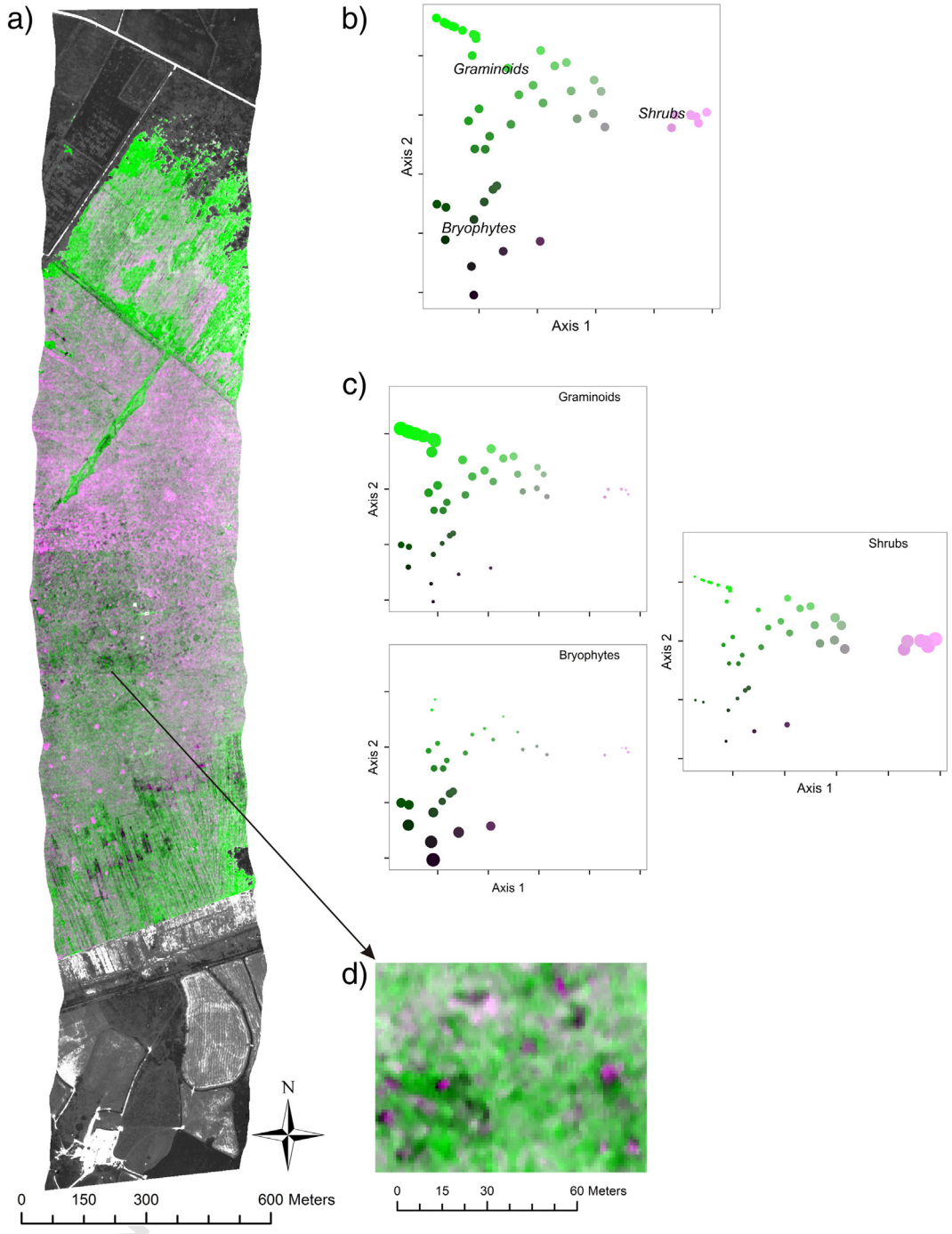

Fig. 8. a) Map of ordination scores representing transitions in peatland plant function type (PFT) (red = axis 1, green = axis 2 and blue = axis 1). Areas surrounding the primary bog are not mapped along with three artificial calibration targets that were also present towards the centre of the image. A normalised difference vegetation index image is used as the background image; b) indicates the position of each PFT in ordination space. The dominant PFT found within each plot is plotted as a centroid and labelled with the PFT name; c) illustrates the proportional coverage of each PFT within each field plot, as indicated by the size of the circle. Plots where the PFT is not present are not shown; and d) a zoom image of a location on the primary bog surface. The colours in the figure represent the plot (b and c) or pixel (a and d) locations in the ordination space; and thus indicates the PFT composition present. (For interpretation of the references to color in this figure legend, the reader is referred to the web version of this article.)

The number of bands selected by the PLSR models for mapping species and PFT transitions was relatively low (16 and 12 respectively), suggesting that hyperspectral data may not be necessary to achieve similar results to those reported here. However, floristic gradients can only be mapped if they cause spatial variation in reflectance (Feilhauer et al., 2013); thus high spatial resolution data will be required for continuous mapping of peatland floristic gradients. Depending on the nature of the peatland surface, high spatial resolution multispectral satellite sensors such as Worldview-II (with a spatial resolution of ~2 m for the 8 multispectral bands and 0.5 m for the panchromatic band) may be useful for mapping peatland PFT transitions. For more localised studies, unmanned aerial vehicles (UAV), which have dramatically lowered in cost over the last decade, show great promise. The very high spatial resolution of the data that can be obtained from a UAV (e.g., <10 cm) will improve the homogeneity of individual pixels and will enable the calculation of detailed spatial statistics relating to surface heterogeneity,

Please cite this article as: Harris, A., et al., Hyperspectral remote sensing of peatland floristic gradients, *Remote Sensing of Environment* (2015), http://dx.doi.org/10.1016/j.rse.2015.01.029

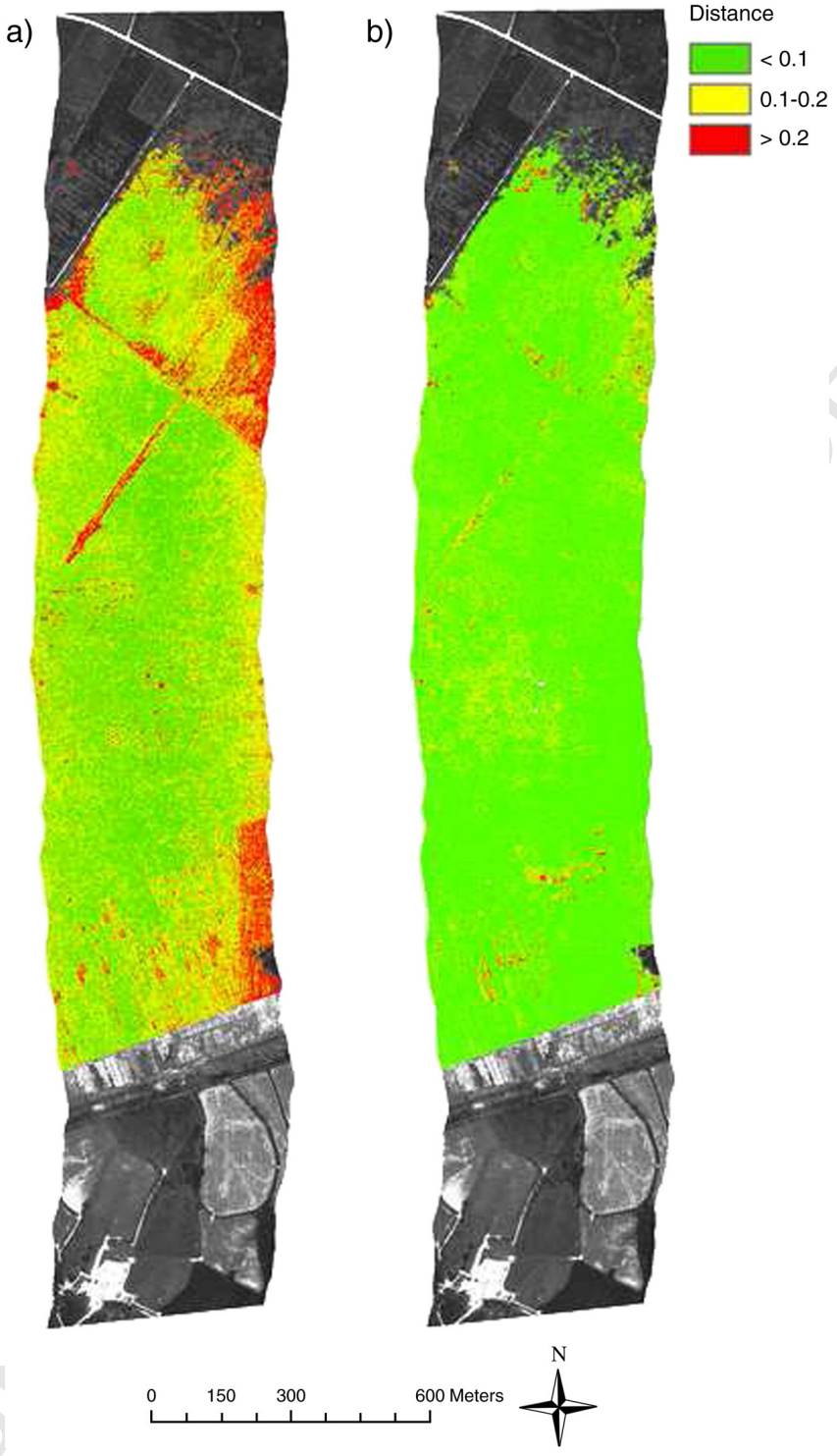

Fig. 9. Map of Euclidean distances between mapped pixels and the nearest-neighbour field sampling plot in Isomap space for a) species level data and b) plant functional type (PFT) data. Green values indicate that a pixel's reflectance is similar to a sampled plot, whereas red pixels indicate the greatest dissimilarities between the image and plot samples and thus indicate greater uncertainty in the model. A normalised difference vegetation index image is used as the background image. (For interpretation of the references to color in this figure legend, the reader is referred to the web version of this article.)

which may improve the quality of mapping and could even partially compensate for lower spectral resolutions. However, little is currently known about the spectral and spatial resolutions required to map PFTs (Ustin & Gamon, 2010), especially at scales that are relevant to the discrimination of peatland ecosystem processes. The optimum level of species aggregation to PFT may also depend on the process being studied (Dorrepaal, 2007).

It is important to recognise that because the ordination–regression approach undertaken in this study is empirical, it is unlikely that the regression coefficients determined for this suite of data in this particular location can be directly transferred to other areas. Environmental gradients and differences in species composition, seasonality and sun-angle viewing geometry greatly influence reflectance but often in ways that are difficult to predict thus field data will be required to supplement

remotely sensed data. However, empirical methods should not be dismissed in the absence of physically-based methods that are able to predict the distribution of complex floristic compositions (Schmidtlein et al., 2012) such as those found in peatland environments. Furthermore, the method outlined in this study does hold advantages over other constrained ordination approaches that have been used to map floristic gradients across peatlands. This is because constrained ordinations, where the ordination axes are forced to be linear combinations of a number of explanatory variables, often require ancillary environmental variables (e.g., moisture and pH), to be measured in situ (Middleton et al., 2012) or use spectral data (Thomas et al., 2002), which can lead to over-fitting due to co-linearity if the number of spectral bands approaches the number of sampled plots.

5. Conclusion

The floristic composition of a peatland can provide important information about the rate and magnitude of environmental processes occurring within. Species level maps of floristic composition can be used to provide suitable data for conservation management, whilst gradient maps of PFTs are more expedite to create and may be related to peatland biogeochemical functions. Our study was the first to use imaging spectrometry together with a combined ordination–regression approach to map assemblages of both species and PFTs across a peatland typical of those found at high latitudes.

Our results suggest that spatially continuous maps of vegetation communities can be obtained from remote sensing data without the need to identify unique spectral signatures for each individual species or PFT. Instead the method relies on the assumption that species and PFTs with similar ecological requirements co-occur and thus will have a similar structure and biochemistry, which results in similar spectral characteristics. However, successful mapping of PFTs in this manner is dependent on how peatland PFTs are defined. The classification of species into existing well-recognised PFTs may not always be the most appropriate grouping from a remote sensing perspective and furthermore, the same definition of PFT may not be useful for elucidating all carbon cycling processes. Consequently further work should focus on understanding how peatland vegetation function and ecological theory can be effectively linked with optical properties.

Although the availability of hyperpsectral data is continuously improving and there are many launches of spaceborne hyperpsectral sensors planned in the near future by both European and US space agencies (e.g., PRISMA, EnMAP and HysplRI); the time taken to obtain and process hyperspectral data is often non-trivial. However, our results suggest that hyperspectral data may not be required to map the spatial patterns of peatland plant communities using the ordination–regression approach. This is despite the similarity in spectral reflectance of many peatland species, which is often the difficulty that many previous methods have struggled to overcome. Sensors that can adequately characterise the red, red-edge and NIR regions of the spectrum may hold great potential for mapping PFT transitions. However, a key assumption of floristic gradient mapping approaches, such as the one used in the study, is that the spatial resolution of the imagery used is of an appropriate resolution with respect to the floristic patterns to be mapped. Consequently, further work is needed to understand the spectral and spatial resolutions required to map peatland vegetation and vegetation function using remote sensing data, at scales that are relevant for discriminating peatland ecological processes and patterns of most importance.

Acknowledgements

We wish to thank Mike Bailey (Natural Resources Wales) for granting access to the Cors Fochno study site. Andy Carr is thanked for his fieldwork assistance. Hannes Feilhauer is also thanked for his help with some of the R coding. The work was supported by a grant from the Natural Environment Research Council Airborne Research & Survey Facility [grant number GB08_12] awarded to Angela Harris. The three anonymous reviewers are also thanked for their constructive comments, which helped improve the manuscript.

References

Belyea, L. R., & Malmer, N. (2004). Carbon sequestration in peatland: Patterns and mechanisms of response to climate change. *Global Change Biology*, *10*, 1043–1052.
Bubier, J. L. (1995). The relationship of vegetation to methane emission and hydrochemical gradients in northern peatlands. *Journal of Ecology*, *83*, 403–420.
Bubier, J. L., Moore, T. R., & Bledzki, L. A. (2007). Effects of nutrient addition on vegetation and carbon cycling in an ombrotrophic bog. *Global Change Biology*, *13*, 1168–1186.
Bubier, J. L., Moore, T. R., & Crosby, G. (2006). Fine-scale vegetation distribution in a cool temperate peatland. *Canadian Journal of Botany—Revue Canadienne De Botanique*, *84*, 910–923.
Bubier, J. L., Rock, B. N., & Crill, P. M. (1997). Spectral reflectance measurments of boreal wetland and forest mosses. *Journal of Geophysical Research*, *102*, 29483–29494.
Chong, I. G., & Jun, C. H. (2005). Performance of some variable selection methods when multicollinearity is present. *Chemometrics and Intelligent Laboratory Systems*, *78*, 103–112.
Cole, B., McMorrow, J., & Evans, M. (2014). Empirical modelling of vegetation abundance from airborne hyperspectral data for upland peatland restoration monitoring. *Remote Sensing*, *6*, 716–739.
De'ath, G. (1999). Extended dissimilarity: A method of robust estimation of ecological distances from high beta diversity data. *Plant Ecology*, *144*, 191–199.
Dias, A. T. C., Hoorens, B., Van Logtestijn, R. S. P., Vermaat, J. E., & Aerts, R. (2010). Plant species composition can be used as a proxy to predict methane emissions in peatland ecosystems after land-use changes. *Ecosystems*, *13*, 526–538.
Díaz, S., & Cabido, M. (2001). Vive la différence: Plant functional diversity matters to ecosystem processes. *Trends in Ecology & Evolution*, *16*, 646–655.
Dorrepaal, E. (2007). Are plant growth-form-based classifications useful in predicting northern ecosystem carbon cycling feedbacks to climate change? *Journal of Ecology*, *95*, 1167–1180.
Dorrepaal, E., Cornelissen, J. H. C., Aerts, R., Wallen, B., & Van Logtestijn, R. S. P. (2005). Are growth forms consistent predictors of leaf litter quality and decomposability across peatlands along a latitudinal gradient? *Journal of Ecology*, *93*, 817–828.
Feilhauer, H., Faude, U., & Schmidtlein, S. (2011). Combining Isomap ordination and imaging spectroscopy to map continuous floristic gradients in a heterogeneous landscape. *Remote Sensing of Environment*, *115*, 2513–2524.
Feilhauer, H., Thonfeld, F., Faude, U., He, K. S., Rocchini, D., & Schmidtlein, S. (2013). Assessing floristic composition with multispectral sensors—A comparison based on monotemporal and multiseasonal field spectra. *International Journal of Applied Earth Observation and Geoinformation*, *21*, 218–229.
Foster, D. R., H.E.W., Jr., Thelaus, M., & King, G. A. (1993). Bog development and landform dynamics im central Sweden and south-eastern Labrador, Canada. *Journal of Ecology*, *76*, 1164–1185.
Gitay, H., & Noble, I. R. (1997). What are functional types and how should we seek them? In T. M. Smith, H. H. Shugart, & F. I. Woodward (Eds.), *Plant functional types: Their relevance to ecosystem properties and global change* (pp. 3–19). Cambridge Univ. Press.
Gorham, E. (1991). Northern peatlands: Role in the carbon cycle and probable responses to climatic warming. *Ecological Applications*, *1*, 182–195.
Gower, J. C. (1966). Some distance properties of latent root and vector methods used in multivariate analysis. *Biometrika*, *53*, 325-&amp.
Gray, A., Levy, P. E., Cooper, M. D. A., Jones, T., Gaiawyn, J., Leeson, S. R., et al. (2013). Methane indicator values for peatlands: A comparison of species and functional groups. *Global Change Biology*, *19*, 1141–1150.
Green, A. A., Berman, M., Switzer, P., & Craig, M. D. (1988). A transformation for ordering mulitpsectral data in terms of image quality with implications for noise removal. *IEEE Transactions on Geoscience and Remote Sensing*, *26*, 65–74.
Grime, J. P. (1974). Vegetation classification by reference to strategies. *Nature*, *250*, 26–31.
Harris, A., & Bryant, R. G. (2009). Northern peatland vegetation and the carbon cycle: A remote sensing approach. In A. J. Baird, L. R. Belyea, X. Comas, A. Reeve, & L. Slater (Eds.), *Carbon cycling in northern peatlands* (pp. 79–98). Washington DC, USA: American Geophysical Union.
Harris, A., Bryant, R. G., & Baird, A. J. (2005). Detecting water stress in *Sphagnum* spp. *Remote Sensing of Environment*, *97*, 371–381.
Harris, A., Bryant, R. G., & Baird, A. J. (2006). Mapping the effects of water stress on *Sphagnum*: Preliminary observations using airborne remote sensing. *Remote Sensing of Environment*, *100*, 363.
Hearn, S. M., Healey, J. R., McDonald, M. A., Turner, A. J., Wong, J. L. G., & Stewart, G. B. (2011). The repeatability of vegetation classification and mapping. *Journal of Environmental Management*, *92*, 1174–1184.
Huemmrich, K. F., Gamon, J. A., Tweedie, C. E., Campbell, P. K. E., Landis, D. R., & Middleton, E. M. (2013). Arctic tundra vegetation functional types based on photosynthetic physiology and optical properties. *IEEE Journal of Selected Topics in Applied Earth Observations and Remote Sensing*, *6*, 265–275.
Kuiper, J. J., Mooij, W. M., Bragazza, L., & Robroek, B. J. M. (2014). Plant functional types define magnitude of drought response in peatland CO_2 exchange. *Ecology*, *95*, 123–131.
Mahecha, M. D., Martinez, A., Lischeid, G., & Beck, E. (2007). Nonlinear dimensionality reduction: Alternative ordination approaches for extracting and visualizing biodiversity patterns in tropical montane forest vegetation data. *Ecological Informatics*, *2*, 138–149.
Mahecha, M. D., & Schmidtlein, S. (2008). Revealing biogeographical patterns by nonlinear ordinations and derived anisotropic spatial filters. *Global Ecology and Biogeography*, *17*, 284–296.

Please cite this article as: Harris, A., et al., Hyperspectral remote sensing of peatland floristic gradients, *Remote Sensing of Environment* (2015), http://dx.doi.org/10.1016/j.rse.2015.01.029

Matthew, M. W., Adler-Golden, S. M., Berk, A., Richtsmeier, S. C., Levine, R. Y., Bernstein, L. S., et al. (2000). Status of atmospheric correction using a MODTRAN4-based algorithm. *SPIE proceedings, algorithms for multispectral, hyperspectral, and ultraspectral imagery VI* (pp. 199–207).

Mehmood, T., Liland, K. H., Snipen, L., & Sæbø, S. (2012). A review of variable selection methods in Partial Least Squares Regression. *Chemometrics and Intelligent Laboratory Systems*, *118*, 62–69.

Middleton, M., Närhi, P., Arkimaa, H., Hyvönen, E., Kuosmanen, V., Treitz, P., et al. (2012). Ordination and hyperspectral remote sensing approach to classify peatland biotopes along soil moisture and fertility gradients. *Remote Sensing of Environment*, *124*, 596–609.

Minchin, P. R. (1987). An evalutaion of the relatice robustness of techniques for ecological ordination. *Vegetatio*, *69*, 89–107.

Minkkinen, K., Korhonen, R., Savolainen, I., & Laine, J. (2002). Carbon balance and radiative forcing of Finnish peatlands 1900–2100 — The impact of forestry drainage *Global Change Biology*, *8*, 785–799.

Oksanen, J., Blanchet, G., Kindt, R., Legendre, P., Minchin, P. R., O'Hara, B., et al. (2013). *vegan: Community ecology package.* R package version 2.0-10 (In).

R Development Core Team (2012). *R: A language and environment for statistical computing.* Vienna, Austria: R Foundation for Statistical Computing (ISBN 3-900051-07-0, http://www.R-project.org/).

Roberts, D. A., Smith, M. O., & Adams, J. B. (1993). Green vegetation, nonphotosynthetic vegetation and soils in AVIRIS data. *Remote Sensing of Environment*, *44*, 255–269.

Rydin, H., & Jeglum, J. K. (2006). *The biology of peatlands — Peatland habitats* New York: Oxford Universtity Press.

Schaepman-Strub, G., Limpens, J., Menken, M., Bartholomeus, H. M., & Schaepman, M. E. (2009). Towards spatial assessment of carbon sequestration in peatlands: Spectroscopy based estimation of fractional cover of three plant functional types. *Biogeosciences*, *6*, 275–284.

Schmidtlein, S., Feilhauer, H., & Bruelheide, H. (2012). Mapping plant strategy types using remote sensing. *Journal of Vegetation Science*, *23*, 395–405.

Schmidtlein, S., & Sassin, J. (2004). Mapping of continuous floristic gradients in grasslands using hyperspectral imagery. *Remote Sensing of Environment*, *92*, 126–138.

Schmidtlein, S., Zimmermann, P., Schüpferling, R., & Weiß, C. (2007). Mapping the floristic continuum: Ordination space position estimated from imaging spectroscopy. *Journal of Vegetation Science*, *18*, 131–140.

Q7 Simpson, E. H. (1949). Measurement of diversity. *Nature*, *163*, 688-688.

Sloan, V. L., Fletcher, B. J., Press, M. C., Williams, M., & Phoenix, G. K. (2013). Leaf and fine root carbon stocks and turnover are coupled across Arctic ecosystems. *Global Change Biology*, *19*, 3668–3676.

Strack, M., & Waddington, J. M. (2007). Response of peatland carbon dioxide and methane fluxes to a water table drawdown experiment. *Global Biogeochemical Cycles*, *21*. http://dx.doi.org/10.1029/2006GB002715.

Tenenbaum, J. B., de Silva, V., & Langford, J. C. (2000). A global geometric framework for nonlinear dimensionality reduction. *Science*, *290*, 2319–2323.

Thessler, S., Ruokolainen, K., Tuomisto, H., & Tomppo, E. (2005). Mapping gradual landscape-scale floristic changes in Amazonian primary rain forests by combining ordination and remote sensing. *Global Ecology and Biogeography*, *14*, 315–325.

Thomas, V., Treitz, P., Jelinski, D., Miller, J., Lafleur, P., & McCaughey, J. H. (2002). Image classification of a northern peatland complex using spectral and plant community data. *Remote Sensing of Environment*, *84*, 83.

Tilman, D., Knops, J., Wedin, D., Reich, P., Ritchie, M., & Siemann, E. (1997). The influence of functional diversity and composition on ecosystem processes. *Science*, *277*, 1300–1302.

Turner, W., Spector, S., Gardiner, N., Fladeland, M., Sterling, E., & Steininger, M. (2003). Remote sensing for biodiversity science and conservation. *Trends in Ecology & Evolution*, *18*, 306–314.

Ustin, S. L., & Gamon, J. A. (2010). Remote sensing of plant functional types. *New Phytologist*, *186*, 795–816.

van Wijk, M. T., Clemmensen, K. E., Shaver, G. R., Williams, M., Callaghan, T. V., Chapin, F. S., et al. (2004). Long-term ecosystem level experiments at Toolik Lake, Alaska, and at Abisko, Northern Sweden: generalizations and differences in ecosystem and plant type responses to global change. *Global Change Biology*, *10*, 105–123.

Waddington, J. M., Griffis, T. J., & Rouse, W. R. (1998). Northern Canadian wetlands: Net ecosystem CO_2 exchange and climate change. *Climatic Change*, *40*, 267–275.

Walker, M. D., Wahren, C. H., Hollister, R. D., Henry, G. H. R., Ahlquist, L. E., Alatalo, J. M., et al. (2006). Plant community responses to experimental warming across the tundra biome. *Proceedings of the National Academy of Sciences of the United States of America*, *103*, 1342–1346.

Ward, S. E., Bardgett, R. D., McNamara, N. P., & Ostle, N. J. (2009). Plant functional group identity influences short-term peatland ecosystem carbon flux: Evidence from a plant removal experiment. *Functional Ecology*, *23*, 454–462.

Wiedermann, M. M., Nordin, A., Gunnarsson, U., Nilsson, M. B., & Ericson, L. (2007). Global change shifts vegetation and plant–parasite interactions in a boreal mire. *Ecology*, *88*, 454–464.

Wold, S., Ruhe, A., Wold, H., & Dunn, W. J. (1984). The collinearity problem in linear-regression — The partial least-squares (PLS) approach to generalized inverses. *Siam Journal on Scientific and Statistical Computing*, *5*, 735–743.

Yu, Z., Loisel, J., Brosseau, D. P., Beilman, D. W., & Hunt, S. J. (2010). Global peatland dynamics since the Last Glacial Maximum. *Geophysical Research Letters*, *37*.

Please cite this article as: Harris, A., et al., Hyperspectral remote sensing of peatland floristic gradients, *Remote Sensing of Environment* (2015), http://dx.doi.org/10.1016/j.rse.2015.01.029